

*Work supported by the U. S. Atomic Energy Commission.

¹J. H. Friedman, S. Steppel, and J. W. Tukey, Stanford Linear Accelerator Center, Computation Group Technical Memo No. 153, 1973 (unpublished).

²J. H. Friedman, Stanford Linear Accelerator Center, Computation Group Technical Memo No. 154, 1973 (unpublished).

³The six-pronged events resulting from a proton exposure in the Brookhaven National Laboratory 80-in. H_2 bubble chamber were fitted to the reaction $pp \rightarrow pp\pi^+\pi^+\pi^-\pi^-$ in the beam momentum range 12–28 GeV/c. For a detailed description of the experiment see D. B. Smith, Ph.D. thesis, Lawrence Berkeley Laboratory Report No. UCRL-20632, 1971 (unpublished).

⁴W. T. Eadie, D. Drijard, F. E. James, M. Roos, and B. Sadoulet, *Statistical Methods in Experimental Physics* (North-Holland, Amsterdam, 1971), p. 257.

⁵For the analyses on these data, identical particles were distinguished by the value of their longitudinal momenta.

⁶The data are really five-dimensional in this subspace

because longitudinal momentum conservation requires all of these data points to lie on a five-dimensional linear manifold within the six-dimensional space.

⁷R. P. Feynman, *Phys. Rev. Lett.* **23**, 1415 (1969).

⁸The data are really ten-dimensional in this subspace because transverse-momentum conservation requires all of these data points to lie on a ten-dimensional linear manifold within the twelve-dimensional space.

⁹P. M. Lewis, *IEEE Trans. Inf. Theory* **IT-8** 171 (1962).

¹⁰This minimum value for the MI estimate expected for the null hypothesis depends upon the sample size and approaches zero asymptotically.

¹¹For these tests, the data from the higher momentum samples (18 to 28 GeV/c) were combined into a single sample of 970 events with mean beam momentum 23 GeV/c.

¹²A standardized variable is one whose expected mean is zero and whose expected variance is unity.

¹³K. B. Wilson, *Acta Phys. Austr.* **17**, 37 (1963).

¹⁴J. H. Friedman, C. Risk, and D. B. Smith, *Phys. Rev. Lett.* **28**, 191 (1971).

Parametrization of multiplicities through the eikonal approximation*

J. St. Amand and R. A. Uritam

Department of Physics, Boston College, Chestnut Hill, Massachusetts 02167

(Received 17 October 1973)

We present an empirical parametrization of the variation in charged secondary multiplicity in high-energy proton-proton collisions with impact parameter through use of the eikonal approximation and general quasi-intuitive arguments. For the domain where proton constituents interact collectively, we obtain the low-order moments of the charged secondary multiplicity distribution.

Recent experimental results¹ at ultrahigh CERN ISR and NAL energies have coincided with and have reinforced the emergence of a simple picture of hadron structure and of heuristic methods for parametrizing hadron phenomena. The simplest of such models visualizes "constituents within constituents,"² or "successive layers of matter,"³ both of which have characteristic dimensions that define the energy scale of the appropriate domain.

Among "simple" methods, the eikonal approximation has received renewed attention recently in the work of Barshay,⁴ Chao and Yang,⁵ and others.⁶ We showed earlier⁷ how, using only the eikonal approximation and the uncertainty relation, one could parametrize the variation of the rms transverse momentum of emitted particles in hadron-hadron collisions with particle size and incident momentum. Here we parametrize the multiplicity using the same heuristic picture.

We confine ourselves to energies where the hadron constituents participate collectively,⁸ so that

the collision probes an extended particle with no structure. Thus, we consider it to be described by a continuous distribution of hadronic matter. Many reasonable fits to this distribution have been used, such as Gaussian or Yukawa shapes. In the heuristic spirit, we try to use the simplest possible assumptions, so we choose a step-function distribution; in short, we are considering homogeneous spheres.⁹

Consider two protons, each of "radius" R . When these approach one another with an impact parameter, $b > 2R$, no production processes take place. For the case, $b < 2R$, we employ again the simplest possible description, in this case the eikonal approximation.⁹ Production of secondaries takes place in the volume overlap of the two interpenetrable spheres that are pictured as moving through one another (Fig. 1). In the notation of Fig. 1, the z axis passes through the center of the target and the projectile moves in the z direction at an impact parameter b . The relative production prob-

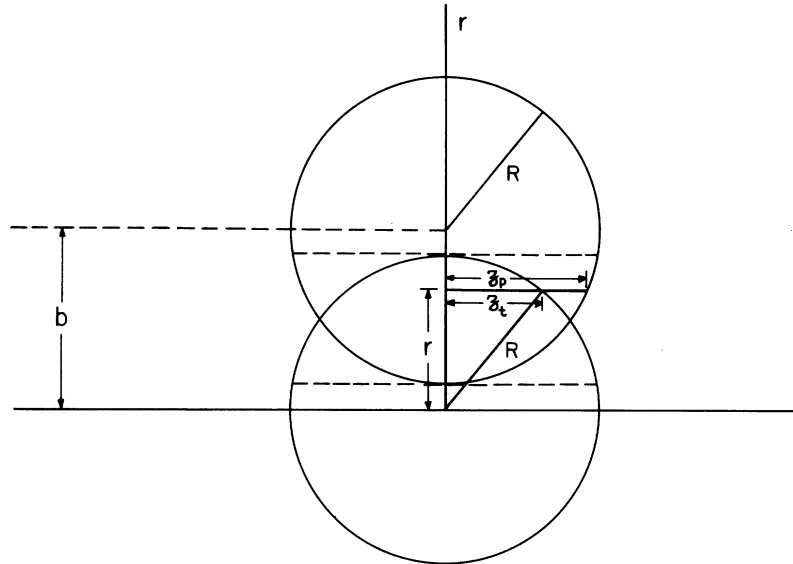


FIG. 1. Geometrical relationships for two spheres of radius R that pass through one another; diagram shows spheres at instant of maximum overlap.

ability is given by the density overlap function,

$$\begin{aligned}
 W(b) &= \int \int z_t(r, \theta) z_p(r, \theta) r dr d\theta, \\
 &= \int \int (R^2 - r^2)^{1/2} (R^2 - b^2 + 2br \cos \theta - r^2)^{1/2} \\
 &\quad \times r dr d\theta, \tag{1}
 \end{aligned}$$

where $z_t(r, \theta)$ and $z_p(r, \theta)$ are half-lengths of the target and of the projectile traversed at (r, θ) . The integral is over the almond-shaped area, normal to the beam direction, bounded by arcs of the circles $r = R$ and $r = b \cos \theta - (R^2 - b^2 \sin^2 \theta)^{1/2}$. A straightforward integration¹⁰ yields

$$\begin{aligned}
 W(b) \propto (4R^4 - b^2) \left[\pi R^2 - \frac{1}{2} b (4R^2 - b^2)^{1/2} \right. \\
 \left. - 2R^2 \sin^{-1}(b/2R) \right]. \tag{2}
 \end{aligned}$$

In experiment one finds that for a fixed incident energy the multiplicity varies from 2 to a certain energy-dependent maximum value (defined such that the cross section for production of a greater number of particles is less than, typically, 0.05 mb).

Using the above ultraheuristic picture we can parametrize the variation in the number of secondaries produced with the impact parameter in the following way. Given a certain energy E , there is a well-defined maximum secondary multiplicity, $n_m(E)$; this value of n is achieved for total overlap of the colliding spheres, i.e., for $b = 0$. At the other extreme, for zero overlap, $n = 0$. Between these, larger values of n are correlated with smaller b values, and hence with greater overlap,

in such a way that equal (integral) increments of n result from equal increments of $W(b)$; i.e., a given multiplicity can occur only for the appropriate value of the density overlap function $W(b)$, and for the corresponding range in b .

Since experiments consider, generally, only charged multiplicities, we specialize to that case, in which n can change only by multiples of 2. Our assumption relates n to a range in b :

n	Range of b
0	$b > b_0$
2	$b_0 \geq b \geq b_2$
⋮	
n	$b_{n-2} \geq b \geq b_n$
⋮	
n_m	$b_{n_m-2} \geq b \geq b_{n_m}$

where $b_0 = 2R$ and $b_{n_m} = 0$. By hypothesis, we set

$$\begin{aligned}
 W(b_0) &= 0, \\
 W(b_2) &= 2\epsilon, \\
 &\vdots \\
 W(b_n) &= n\epsilon, \\
 &\vdots \\
 W(b_{n_m}) &= n_m \epsilon, \tag{4}
 \end{aligned}$$

where ϵ is a constant.

One can immediately solve for the b_n , using Eq. (2):

$$W(b_n) = \frac{n}{n_m} W(0). \quad (5)$$

Since a given multiplicity, n , occurs only when $b_{n-2} \geq b \geq b_n$, the relative probability for this multiplicity is

$$f_n = \frac{1}{4R^2} (b_{n-2}^2 - b_n^2). \quad (6)$$

The values of the impact parameter are of course not subject to experimental control or measurement; however, one can calculate from this model the average charged secondary multiplicity, as well as the higher moments of the distribution.

Concentrating first on the mean as the most straightforward measure of the distribution, by using values of b_n determined from Eqs. (5), we have

$$\langle n \rangle = \frac{1}{4R^2} \sum_{n=2}^{n_m} n(b_{n-2}^2 - b_n^2). \quad (7)$$

Recent experiments with pp collisions at incident momenta of 102 GeV/c,^{11,12} 205 GeV/c,¹³ 303 GeV/c,¹⁴ and 405 GeV/c¹² yield maximum secondary multiplicities of 16, 20, 24, and 24, respectively.¹⁵ Table I presents $\langle n \rangle$ for these cases, from experiment and from Eq. (7).

Agreement improves with increasing energy; thus we have also calculated $\langle n \rangle$ for very high maximum secondary multiplicities of 40 and 50. A recent ISR experiment¹⁶ at the highest ISR energies ($s \sim 2800$ GeV²) indicates an average charged secondary multiplicity of ~ 10.3 . We conjecture

TABLE I. Average charged secondary multiplicities in pp collisions.

Maximum charged secondary multiplicity	Average charged secondary multiplicity	Average charged secondary multiplicity
n_m	$\langle n \rangle$ (theory)	$\langle n \rangle$ (experiment)
16	4.30	3.60
20	5.02	4.70
24	5.80	5.60
40	8.68	$\sim 10.3^a$
50	10.56	$\sim 10.3^a$

^a See Ref. 16 and remarks in text.

that in the asymptotic limit of the hadron domain⁸ the present scheme converges to the correct charged secondary multiplicity. At even higher energies, where hadronic constituents^{2,3} participate individually in collisions, the foregoing is not a complete picture; contributions to production from individual constituents must also be considered.

Table II presents a tabulation of other low-order moments¹⁷ of the multiplicity distribution, as calculated from the model and from experiment. The higher moments are of course more severe tests of a model, and agreement with experiment is harder to achieve. While our computed values are not spectacularly successful for third- and fourth-order moments, they are quite reasonable

TABLE II. Low-order moments of the charged secondary multiplicity distribution.

	102 GeV/c		205 GeV/c		303 GeV/c		405 GeV/c
	Theory	Exp.	Theory	Exp.	Theory ^c	Exp. ^c	Exp. ^c
$\langle n^2 \rangle$	30.31	23.16	45.86	39.11	54.52	54.14	57.36
$D = (\langle n^2 \rangle - \langle n \rangle^2)^{1/2}$	3.41	3.26	4.36	4.13	4.57	4.77	5.05
$\langle n \rangle / D$	1.27	1.09	1.19	1.14	1.27	1.17	1.12
$g_2 = \langle n(n-1) \rangle$	25.99	19.62	40.68	34.42	49.22	46.78	51.72
$f_2 = g_2 - f_1^2$	7.33	7.09	13.85	12.33	15.58	15.42	19.91
g_3^a	208.15	120.43	423.07	285.14	699.79	482.14	531.67
f_3^a	32.53	9.77	58.85	7.47	236.5	47.47	15.4
g_4^a	1814	785	4773	2556	9785	5257	...
f_4^a	-78.4	-66.7	-59.4	-162.6	-651	-404	...
$\left(\frac{f_2 + \langle n \rangle}{\langle n \rangle^2} \right)^b$	0.62	0.85	0.71	0.77	0.64	0.67	0.18

^a $g_3 = \langle n(n-1)(n-2) \rangle$, $f_3 = g_3 - 3f_1f_2 - f_1^3$, $g_4 = \langle n(n-1)(n-2)(n-3) \rangle$, $f_4 = g_4 - 6f_1^2f_2 - 3f_2^2 - 4f_1f_3 - f_1^4$; see Ref. 17.

^b A combination of Mueller correlation parameters, predicted to be constant; see Ref. 17.

^c The theoretical results are the same for 303 and 405 GeV/c, and the experimental results are preliminary for the latter case. See Ref. 15.

for all moments through the second order, and even for the higher moments agreement improves with increasing energy, so again we would suggest agreement in this limit.

In terms of a "layered structure"³ of the proton itself we can correlate the values of b_n , where the multiplicity changes, with the corresponding "radius" of the target, r_n , to which the projectile has penetrated, by noting the reasonable definition

$$b_n = R + r_n. \quad (8)$$

Using the usual value $R = 0.9$ fm,¹⁸ we have at the highest energies $r_2 = 0.43$ fm and $r_4 = 0.27$ fm. This agrees closely with other related calculations of nucleon layer radii.¹⁸

We can remark qualitatively on πp collisions in terms of this model. If we assume that $r_n < r_p$,¹⁹ then at small b values further decrease of b will not cause the overlap function to increase as fast⁷ as for spheres of equal radii. Hence b must change faster in this region, so in computing $\langle n \rangle$ through Eq. (7) high n values are now weighted by larger coefficients ($b_{n-2}^2 - b_n^2$); thus $\langle n \rangle$ is increased. Indeed, we see from experiment, comparing $p p$ (Ref. 13) and πp (Ref. 20) collisions at

205 GeV/c, that $\langle n \rangle$ and other first-order moments are slightly higher for πp .

The entire development depends on taking $n_m(E)$ as a given quantity and finding the moments on the basis of this. However, beyond that, the result is a universal parametrization free of any other numerical parameters. Thus, while no one would consider (nor do we propose) this scheme as a complete literal theory of hadron structure and of the production mechanism, nevertheless the thoroughgoing simplicity and quasi-intuitive nature of the picture, together with modest success in parametrization, points toward a more serious consideration of the nature of "intuitive" vs. "abstract" schemes for hadron structure. Elsewhere²¹ we present further computational details and take up the idea that such an approach may yield as complete an account as one is likely to get of the asymptotic limit of a domain of hadron phenomena dominated by the characteristic length—whether of the hadron or of its constituents.

We are indebted to Professor L. Van Hove for some helpful remarks and to Dr. P. Nuthakki for useful discussions during early phases of this work.

*Work supported in part by the U. S. National Aeronautics and Space Administration under Grant No. NAS 9-4065.

¹For example, M. Jacob, in *Proceedings of the XVI International Conference on High Energy Physics, Chicago-Batavia, Ill., 1972*, edited by J. D. Jackson and A. Roberts (NAL, Batavia, Ill., 1973), Vol. 3, p. 373; B. Alper *et al.*, Phys. Lett. 44B, 521 (1973); 44B, 527 (1973); M. Banner *et al.*, *ibid.* 44B, 537 (1973); F. W. Büsser *et al.*, *ibid.* 46B, 471 (1973); J. W. Cronin *et al.*, Phys. Rev. Lett. 31, 1426 (1973).

²R. P. Feynman, Phys. Rev. Lett. 23, 1415 (1969); P. V. Landshoff and J. C. Polkinghorne, Phys. Lett. 5C, 1 (1972); S. M. Berman, J. D. Bjorken, and J. B. Kogut, Phys. Rev. D 4, 3388 (1971); T. D. Lee and S. D. Drell, *ibid.* 5, 1738 (1972); S. D. Drell and K. Johnson, *ibid.* 6, 3248 (1972).

³M. S. Chanowitz and S. D. Drell, Phys. Rev. Lett. 30, 807 (1973); G. Eilam and Y. Gell, Phys. Rev. D 8, 168 (1973); M. M. Islam and J. Rosen, Phys. Rev. Lett. 22, 502 (1969).

⁴S. Barshay, Phys. Lett. 42B, 475 (1972); Nuovo Cimento Lett. 7, 671 (1973).

⁵A. Wu Chao and C. N. Yang, Phys. Rev. D 8, 2063 (1973).

⁶H. Moreno, Phys. Rev. D 8, 268 (1973); A. D. Krisch, Phys. Lett. 44B, 71 (1973); B. J. Kirby and H. M. Fried, Phys. Rev. D 8, 2668 (1973); D. Agassi and A. Gal, Phys. Rev. Lett. 31, 961 (1973); R. Blankenbecler, J. R. Fulco, and R. L. Sugar, Phys. Rev. D 9, 736 (1974).

⁷J. St. Amand and R. A. Uritam, Nuovo Cimento 17A, 493 (1973).

⁸Berman *et al.*, Ref. 2; F. Halzen, Wisconsin Report No. C00-361 (unpublished).

⁹R. Serber, Rev. Mod. Phys. 36, 649 (1964); S. Fernbach, R. Serber, and T. B. Taylor, Phys. Rev. 75, 1352 (1949); R. J. Glauber, in *Lectures in Theoretical Physics*, edited by W. E. Brittin and L. B. Dunham (Interscience, New York, 1959), Vol. I.

¹⁰St. Amand and Uritam, Ref. 7. In that work we used $W(b)$ as a weighting factor to compute the rms distance from the z axis at which production originates, namely

$$\langle r^2 \rangle = \frac{\int_0^{2\pi} \int_0^{2R} r^2(b) W(b) b db d\theta}{\int_0^{2\pi} \int_0^{2R} W(b) b db d\theta};$$

the quantity $\Delta x_T = \langle r^2 \rangle^{1/2}$ is the variable conjugate to the rms transverse momentum.

¹¹J. W. Chapman *et al.*, Phys. Rev. Lett. 29, 1686 (1972).

¹²C. Bromberg *et al.*, Phys. Rev. Lett. 31, 1563 (1973).

¹³G. Charlton *et al.*, Phys. Rev. Lett. 29, 515 (1972).

¹⁴F. T. Dao *et al.*, Phys. Rev. Lett. 29, 1627 (1972).

¹⁵The maximum secondary multiplicity at 405 GeV/c is the same as at 303 GeV/c if we adhere to the definition of n_m by which $\sigma < 0.05$ mb for $n > n_m$. Indeed this cutoff is not entirely well established from the data for 405 GeV/c (Ref. 12). Since our computation depends sensitively on a well-defined value of n_m , it makes

comparison with experiment problematic, using data at 405 GeV/c.

¹⁶M. Antinucci *et al.*, Nuovo Cimento Lett. **6**, 121 (1973).

¹⁷For definitions of various moments see A. H. Mueller, Phys. Rev. D **4**, 150 (1971); P. Slattery, *ibid.* **7**, 2073 (1973); also Refs. 12 and 14.

¹⁸Eilam and Gell, Ref. 3. For the first two layer boundaries, Eilam and Gell (Ref. 3) obtain 0.44 fm and 0.33 fm. Islam and Rosen (Ref. 3) report 0.44 fm and 0.2 fm, and values of 0.48 fm and 0.32 fm by A. D.

Krisch are quoted (Ref. 3).

¹⁹C. F. Cho and J. J. Sakurai, Nuovo Cimento Lett. **2**, 7 (1971).

²⁰D. Bogart *et al.*, Phys. Rev. Lett. **31**, 1271 (1973).

Here the comparison is made for total charged multiplicity. $\langle n \rangle_{pp} = 7.68 \pm 0.11$; $\langle n \rangle_{\pi p} = 8.02 \pm 0.12$; $\langle n(n-1) \rangle_{pp} = 66.6 \pm 1.4$; $\langle n(n-1) \rangle_{\pi p} = 71.6 \pm 1.8$. At 100 GeV/c, $\langle n \rangle_{pp} = 6.49 \pm 0.10$ and $\langle n \rangle_{\pi+p} = 6.80 \pm 0.14$; see J. Erwin *et al.*, Phys. Rev. Lett. **32**, 254 (1974).

²¹St. Amand and Uritam, Ref. 7 and unpublished work.

Large-transverse-momentum phenomena and Fermi's statistical model for multiparticle production at high energies

Meng Ta-chung

Institut für Theoretische Physik, Freie Universität Berlin, Berlin, Germany

(Received 11 February 1974)

Recent experimental findings at NAL and at the CERN ISR in connection with large-transverse-momentum phenomena are analyzed. It is observed that these data can be understood in the framework of Fermi's statistical model. A new scaling variable is proposed. Further experiments are suggested.

I. INTRODUCTION

Recent measurements at the CERN ISR¹⁻³ and at NAL^{4,5} of inclusive cross sections $E d^3\sigma/dp^3$ at large transverse momentum ($p_T > 1$ GeV/c) and wide center-of-mass angles (θ near 90°) have attracted much attention in the study of multiparticle production processes. In this paper we present the result of an analysis of these data as well as of other experimental findings^{6,7} relevant to the large- p_T phenomena. We show that these data can be understood in the framework of Fermi's statistical model.^{8,9}

The most striking features of the large-transverse-momentum processes are that (a) the wide-angle inclusive cross section $E d^3\sigma/dp^3$ for large p_T is much larger than that expected from the simple extrapolation of the exponential behavior encountered for $p_T < 1$ GeV/c, (b) this cross section increases with increasing total energy \sqrt{s} , (c) the energy dependence of this quantity is small at low p_T but becomes stronger as p_T increases, (d) at fixed energies the cross section at wide angles (θ near 90°) is almost independent of θ , (e) the pions have lost the overwhelming supremacy which they show over all other secondaries at $p_T < 1$ GeV, and (f) the associated multiplicity at wide angles increases with increasing p_T . It has been reported⁶ that the Pisa-Stony Brook group sees an increase of the charged multiplicity

at wide angle when the transverse momentum of a specified wide-angle γ ray is increased. At the same time the multiplicity at small angle (very fast secondaries) drops. The CERN-Columbia-Rockefeller group finds that the charged multiplicity at 90° increases greatly when measurement of a 3-GeV/c π^0 is required. This increase is found not only in the direction opposite to the π^0 (factor 2.5, say) but also in the direction of π^0 (factor 1.8, say). Furthermore, (g) a strong "back-to-back" correlation between large-transverse-momentum π^0 's is found.

Because of the apparent close connection [cf. item (f)] between the production of large- p_T particles and the angular distribution of multiplicities, it seems useful also to study the angular distribution in semi-inclusive processes. Angular distribution data, obtained *only* from processes in which at least one large- p_T particle is observed, are not available. However, such distributions *independent of this restriction* can be obtained from the existing data^{10,6} for the single-particle η distribution at fixed charged multiplicities, $(1/\sigma_n) d\sigma_n/d\eta$. Here $\eta = -\ln \tan(\theta/2)$, n is the charged multiplicity, σ_n is the topological cross section,

$$\frac{1}{\sigma_n} \frac{d\sigma_n}{d\cos\theta} = \cosh^2\eta \left(\frac{1}{\sigma_n} \frac{d\sigma_n}{d\eta} \right), \quad (1)$$

and θ is the c.m. scattering angle. These data^{10,6} are given in Fig. 1. We see that while the forward